JOURNAL OF BONE AND MINERAL RESEARCH
Volume 16, Number 9, 2001

Case Report

Gnathodiaphyseal Dysplasia: A Syndrome of Fibro-Osseous Lesions of Jawbones, Bone Fragility, and Long Bone Bowing

MARA RIMINUCCI,[1,2] MICHAEL T. COLLINS,[3] ALESSANDRO CORSI,[1,2] ALAN BOYDE,[4] MARK D. MURPHEY,[5–7] SHLOMO WIENTROUB,[8] SERGEI A. KUZNETSOV,[3] NATASHA CHERMAN,[3] PAMELA GEHRON ROBEY,[3] and PAOLO BIANCO[2,3]

ABSTRACT

We report an unusual generalized skeletal syndrome characterized by fibro-osseous lesions of the jawbones with a prominent psammomatoid body component, bone fragility, and bowing/sclerosis of tubular bones. The case fits with the emerging profile of a distinct syndrome with similarities to previously reported cases, some with an autosomal dominant inheritance and others sporadic. We suggest that the syndrome be named gnathodiaphyseal dysplasia. The patient had been diagnosed previously with polyostotic fibrous dysplasia (PFD) elsewhere, but further clinical evaluation, histopathological study, and mutation analysis excluded this diagnosis. In addition to providing a novel observation of an as yet poorly characterized syndrome, the case illustrates the need for stringent diagnostic criteria for FD. The jaw lesions showed fibro-osseous features with the histopathological characteristics of cemento-ossifying fibroma, psammomatoid variant. This case emphasizes that the boundaries between genuine GNAS1 mutation–positive FD and other fibro-osseous lesions occurring in the jawbones should be kept sharply defined, contrary to a prevailing tendency in the literature. A detailed pathological study revealed previously unreported features of cemento-ossifying fibroma, including the participation of myofibroblasts and the occurrence of psammomatoid bodies and aberrant mineralization, within the walls of blood vessels. Transplantation of stromal cells grown from the lesion into immunocompromised mice resulted in a close mimicry of the native lesion, including the sporadic formation of psammomatoid bodies, suggesting an intrinsic abnormality of bone-forming cells. (J Bone Miner Res 2001;16: 1710–1718)

Key words: gnathodiaphyseal dysplasia, fibrous dysplasia, craniofacial, craniognathic, bone fragility, fractures, bowing, fibro-osseous, ossifying fibroma, cemento-ossifying fibroma, psammomatoid bodies

[1]Division of Pathology, Department of Experimental Medicine, University of L'Aquila, L'Aquila, Italy.
[2]Division of Pathology, Department of Experimental Medicine and Pathology, University of Rome "La Sapienza," Rome, Italy.
[3]Craniofacial and Skeletal Diseases Branch, National Institute of Dental and Craniofacial Research, National Institutes of Health, Bethesda, Maryland, USA.
[4]Department of Anatomy and Developmental Biology, University College, London, United Kingdom.
[5]Department of Radiologic Pathology, Armed Forces Institute of Pathology, Washington, D.C., USA.
[6]Department of Radiology and Nuclear Medicine, Uniformed Services University of the Health Sciences, Bethesda, Maryland, USA.
[7]Department of Diagnostic Radiology, University of Maryland Medical Center, Baltimore, Maryland, USA.
[8]Department of Pediatric Orthopedic Surgery, Dana Children's Hospital, Tel-Aviv Medical Center, Tel-Aviv, Israel.

INTRODUCTION

FIBROUS DYSPLASIA (FD) is the most common benign fibro-osseous lesion in the jaws.[1–5] FD lesions occurring in the jawbones may be histologically distinctive, but also may exhibit features shared by other less well-defined entities such as ossifying or cemento-ossifying fibromas.[6–11] Based on this partial clinical and pathological overlap, the tendency to group benign fibro-osseous lesions of the jawbones into a single continuous spectrum of lesions has gained widespread acceptance.[12] The very existence of entities deserving the label of ossifying fibroma of the jawbones is questioned by several experts.[12] However, the recognition of a defined (and defining) gene mutation provides an important new dimension to the diagnosis of FD and a potential tool to distinguish between these histologically similar but clinically distinct syndromes.[13–15]

FD of the jawbones is commonly part of polyostotic FD (PFD), whether in combination with endocrinopathies (McCune-Albright syndrome [MAS]) or in their absence.[13,14] PFD results from postzygotic activating mutations (R201C, R201H, and more rarely, other amino acid substitutions) of the GNAS1 gene, encoding the α-subunit of the stimulatory G protein, Gs. Dysfunction of cells in the osteogenic lineage leads to replacement of the normal marrow and bone structure with a characteristic type of abnormal woven bone associated with an abnormal "fibrous" tissue comprised of cells with osteogenic phenotype.[16] Multifocal skeletal lesions, notable for their asymmetric distribution throughout the skeleton, lead to significant deformity and fragility of the affected bones and are clinically expressed with marked changes in biochemical parameters of bone metabolism. Outside of the context of FD/MAS, benign fibro-osseous lesions of the jawbones that occur in conjunction with a systemic skeletal syndrome (such as the hyperparathyroidism-jaw tumor syndrome) are exceedingly rare and often poorly characterized. Here, we report the case of a GNAS1 mutation–negative cemento-ossifying fibroma of the jawbones exhibiting hitherto unrecognized histological features. The lesion occurred within the context of a complex skeletal syndrome of bone fragility and bowing with diaphyseal sclerosis of the long bones, likely fitting into the profile of an emerging clinicopathological entity that we suggest should be called "gnathodiaphyseal dysplasia."

CASE HISTORY

The patient, a 5-year-old white boy, was enrolled in an ongoing study on the natural history of PFD conducted at the National Institutes of Health (NIH protocol 98-D-0145) after a diagnosis of PFD was made elsewhere. He was the child of nonconsanguineous parents with no family history of genetic or skeletal diseases or neurofibromatosis.

He presented at the age of 13 months with bilateral, relatively symmetric, expansile lesions in the maxillary bones associated with a sinus infection. Radiographic examinations at various ages and of various anatomical sites are shown (Fig. 1). In addition to their remarkable symmetry and expansile nature, the maxillary lesions exhibited a degree of lucency with occasional mineralized areas. A complete radiographic survey showed the additional findings of lytic lesions to the right and left of the midline in the mandible. Bowing and cortical thickening of the diaphyseal region of the tibias and fibulae were present. Similar changes also were observed in the right ulna and radius. The spine, femora, and growth plates all appeared normal. A bone scan revealed increased uptake in the maxilla and mandible, normal tracer distribution at the growth plates, and no uptake in the skull base or the tibias.

Incisional biopsy specimens of the right and left maxilla and mandible were initially read as consistent with FD. Subsequent review of the histological material at two major referral centers before enrolling in the NIH study concurred with the original reading of FD. At the age of 14 months, surgical reduction of maxillary lesions was performed, with removal of abnormal tissue and grafting of autologous iliac bone. A similar procedure was subsequently performed for treatment of the mandibular lesions, followed by three further surgeries on the maxillary lesions over the ensuing 3 years.

Over the same time interval, the patient sustained five fractures, all occurring as a result of minimal trauma. Sites of fracture included the left tibia and fibula, both clavicles (three fractures), and the left wrist.

Physical examination at the NIH revealed the symmetrical prominence of the cheeks bilaterally, and bowing of the distal lower extremities, left greater than right. The height and weight were normal for age. He was Tanner stage I and the rest of the physical examination was normal. Specifically, there was no evidence of café-au-lait skin pigmentation, neurofibromas, or Lisch nodules. Sclerae were white and erupted teeth were normal. There was no evidence of scoliosis, hypermobility of the joints, or arched palate. Neither the facial bone lesions nor the lower extremity lesions were painful to palpation.

The Z score of the bone densitometry measurement of the spine by dual-energy X-ray absorptiometry (DXA) was within the normal range. An iliac crest biopsy specimen also was unremarkable on qualitative and quantitative assessment. Specifically, it failed to show a reduced trabecular bone mass as a basis for the bone fragility (percentage of trabecular bone volume [BV/TV%] = 15.4; normal range for age, 13.5–22.9 years). Serum electrolytes, calcium, phosphorus, magnesium, parathyroid hormone, 25- and 1,25-vitamin D, thyroid function tests, and insulin-like growth factor 1 (IGF-1) were normal. Alkaline phosphatase was elevated only minimally (345 U/liter; normal range, 145–320 U/liter). Other markers of bone metabolism including bone-specific alkaline phosphatase, N-telopeptide, and the pyridinium cross-links were within the age-specific normal ranges. Urinary creatinine clearance, calcium, magnesium, tubular maximum reabsorption of phosphorus, and amino acid screen were normal. Karyotype was normal (46,XY).

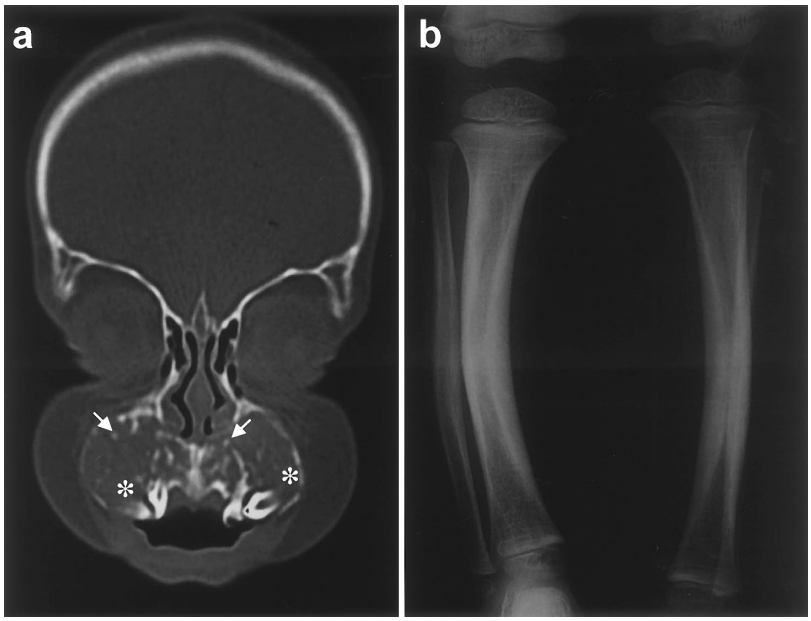

FIG. 1. Radiological findings. A coronal computed tomography (CT) scan with bone windows through the midmaxilla (a) shows bilateral, relatively symmetrical expansile lesions of the maxilla. The lesions are composed predominantly of soft tissue (asterisks) with occasional punctate areas of calcification (arrows). An anteroposterior radiograph of the tibias and fibulae (b) shows diaphyseal cortical thickening and lateral bowing.

MATERIALS AND METHODS

Histology

Fresh pathological tissues were used for cell cultures, mutation analysis, and histological evaluation. Tissues used for histology were fixed with 4% neutral buffered formalin for 2 h at 4°C. After fixation, samples were decalcified with 4% EDTA in phosphate buffer, pH 7, and embedded in paraffin or directly embedded in methylmethacrylate (MMA) without decalcification. Five-micrometer-thick sections from paraffin blocks were used for standard hematoxylin and eosin (H&E) staining and immunohistochemistry; 3- to 5-μm thick sections were cut from MMA blocks and stained with Von Kossa stain.

Backscattered electron imaging

For backscattered electron (BSE) imaging studies, MMA blocks were trimmed, polished, and carbon-coated. BSE imaging and the density of mineralization of the bone tissue were evaluated in a digital SEM (Zeiss DSM 962 with Kontron IBAS external control computer, Zeiss UK Ltd., Welwyn Garden City, Herts, UK) using standardized conditions previously described.[17] A similarly prepared sample of FD bone from our files was studied for comparison.

Bone marrow stromal cell cultures

Bone marrow stromal cell cultures were established as previously described.[18] Briefly, cells were released by scraping fresh bone marrow tissues in nutrient medium that consisted of α-modified minimum essential medium (α-MEM; Life Technologies, Grand Island, NY, USA), 2 mM L-glutamine, 100 U/ml penicillin, 100 μg/ml streptomycin sulfate (Biofluids, Rockville, MD, USA), 20% fetal bovine serum (Equitech-Bio, Inc., Kerrville, TX, USA), 10^{-8} M dexamethasone (Sigma, St. Louis, MO, USA), and 10^{-4} M L-ascorbic acid phosphate magnesium salt (Wako, Osaka, Japan). A single cell suspension was obtained by repeated pipetting and serial passage through needles with decreasing diameter and a 70-μm pore size nylon cell strainer (Becton Dickinson, Franklin Lakes, NJ, USA). Cells were then plated at approximately 0.5×10^5 nucleated cells/cm^2 in 75-cm^2 and 175-cm^2 flasks to generate a high number of colonies. During the first passage, all colonies were combined to obtain a multistrain-derived population.

Mutation analysis

GNAS1 mutation analysis was performed both by standard polymerase chain reaction (PCR) amplification of the relevant target DNA followed by DNA sequencing, or by a polypeptide nucleic acid (PNA)–based DNA sequencing method as previously described.[13] Briefly, genomic DNA (gDNA) was extracted from fresh tissues and cell cultures by the Qiamp Tissue kit (Qiagen, Valencia, CA, USA) according to the manufacturer's instructions. A 300-base pair (bp) fragment of the Gsα gene (GenBank accession number M21142) including the R201 codon was amplified using the following primers: sense, 5′-GTTTCAGGACCTGCTTCGC-3′ (bases 420–438), and antisense, 5′-GCAAAGCCAAGAGCGTGAG-3′ (bases 728–746). A PNA sequence complementary to the wild-type sequence (amino-terminal 5′-CGCTGCCGTGTC carboxy-terminal 3′; bases 436–447) was added to the reaction mixture to prevent the binding of the sense primer to the normal allele. This allowed the selective amplification and sequencing of the mutated allele. The target gDNA was amplified in a standard PCR reaction mixture containing 2 μg PNA. After 15 minutes of denaturation at 94°C, 40 cycles of amplifi-

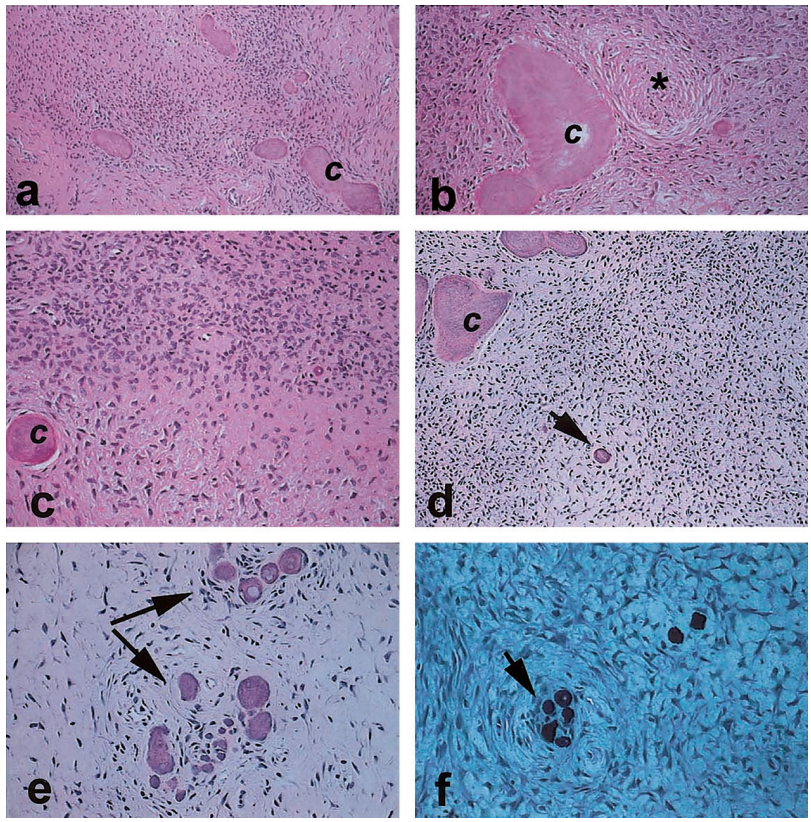

FIG. 2. Histology of the jaw lesion (a–c). Large eosinophilic masses of cementum-like material (*c*) interspersed in a fibrous background with variable cellularity. (d–f) Arrows point to psammomatoid structures. Note that the cementum-like material is acellular. (a–e) H&E-stained paraffin sections. (f) von Kossa staining of undecalcified MMA section. Asterisk in panel b identifies an abnormal hyalinized blood vessel for comparison with Fig. 4.

cation were performed at the following temperatures: 94°C for 30 s, 68°C for 60 s (to allow the binding of the PNA), 55°C for 30 s (to allow the binding of the sense primer), and 72°C for 60 s. The final extension was 7 minutes at 72°C. The PCR product was purified using the Promega Wizard PCR Preps DNA Purification System (Promega, Madison, WI, USA) and then, sequenced using an internal (reverse) primer (5′-CCACGTCAAACATGCTGGTG-3′) by using dRhodamine dye-terminator cycle sequencing with Ampli *Taq* and the Perkin Elmer Applied Biosystem 377 Automated sequencer (Palo Alto, CA, USA).

Immunohistochemistry

Sections from paraffin-embedded tissue were immunostained for α-smooth muscle-specific (α-SM) actin and matrix metalloproteinase 2 (MMP-2/gelatinase A). After deparaffinization, sections were exposed to 3% hydrogen peroxide for 30 minutes to inhibit endogenous peroxidase activity and incubated for 1 h with normal rabbit serum (Dako, Glostrup, Denmark) diluted 1:10 in phosphate-buffered saline (PBS) and 0.1% bovine serum albumin (BSA). Primary antibodies were applied overnight at 4°C at the following concentrations: anti–α-SM actin (clone 1A4 Dako), 1:50; and anti-human MMP-2 (Chemicon International, Temecula, CA, USA), 20 μg/ml. After incubation with primary antibodies, slides were washed four times with PBS and 0.1% Triton X-100 and incubated with biotinylated rabbit anti-mouse immunoglobulin G (IgG; Sigma) diluted 1:200 in PBS and 0.1% BSA for 30 minutes at room temperature. Sections were then washed with PBS and 0.1% Triton X-100 four times and exposed to peroxidase-conjugated extravidin (Sigma) diluted 1:50 in PBS and 0.1% BSA for 30 minutes at room temperature. The peroxidase reaction was developed using 3,3′-diaminobenzidine (DAB) tetrahydrochloride (Sigma) as substrate.

In vivo transplantation assay

Multicolony-derived strains of bone marrow stromal cells were implanted into immunocompromised mice as described previously.[19] Briefly, bone marrow stromal cells were expanded ex vivo, passaged, and cells of the second passage were resuspended in nutrient medium. Cell suspensions were incubated with hydroxyapatite/tricalcium phosphate ceramic powder (Zimmer, Warsaw, IN, USA), to allow the adhesion of cells to ceramic particles, and then implanted into the subcutis of NIH-bg-ν-xidBR (beige) mice (Harlan Sprague–Dawley, Indianapolis, IN, USA). Transplants were harvested at 8 weeks, fixed with 4% buffered formalin, and processed routinely for paraffin embedding.

RESULTS

Mutation analysis

No mutations of the GNAS1 gene were detected on analysis of the amplification product of gDNA from either DNA ex-

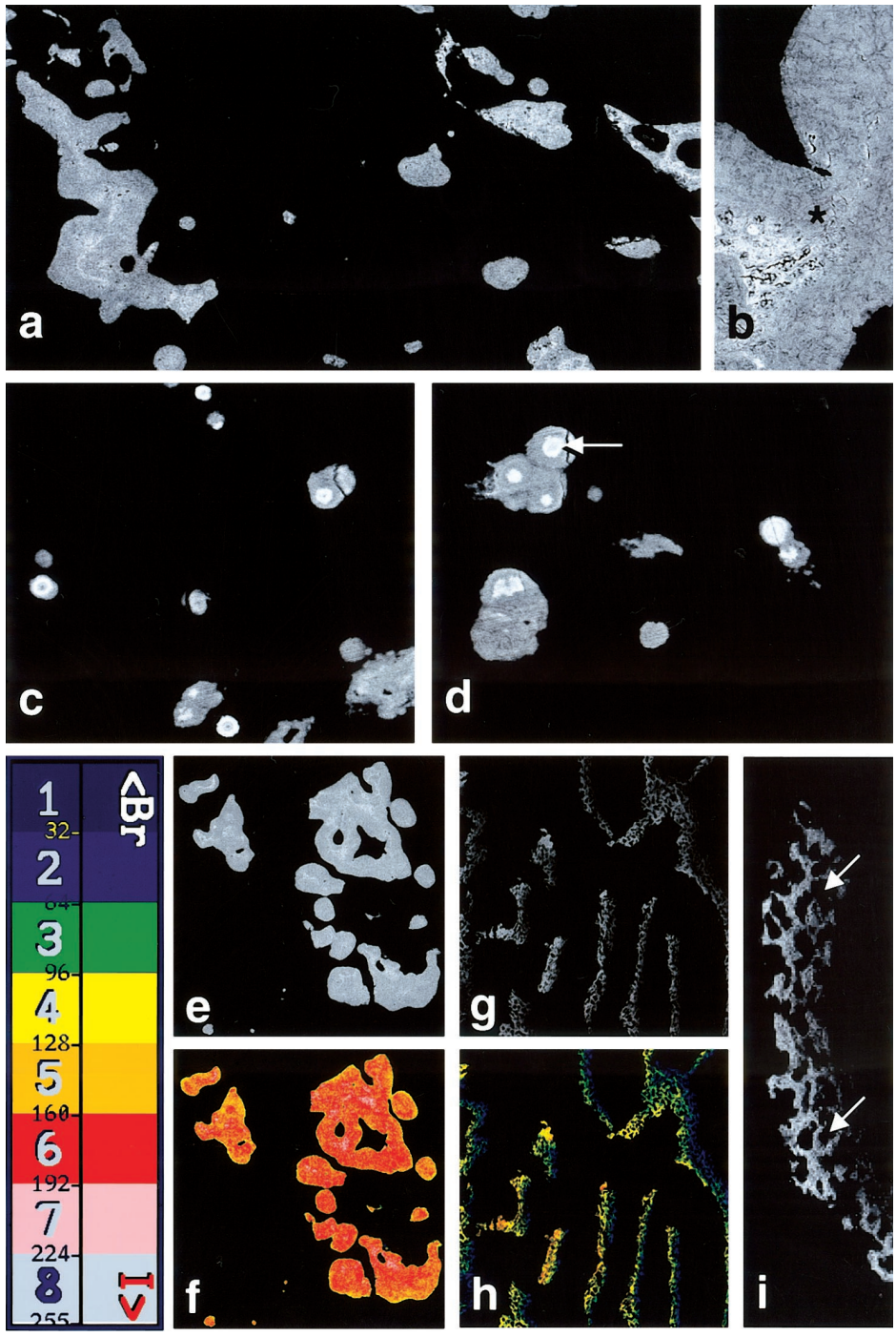

FIG. 3. BSE imaging. Plastic embedded blocks were micromilled, carbon-coated, and studied in a Zeiss DSM962 automated digital SEM at 20 kV and 0.5 nA. (a) Overview of the gnathodiaphyseal syndrome (GDS) lesional tissue showing irregular masses of acellular mineralized material and more minute, rounded mineralized bodies. Whiter areas represent higher mineralization density. (b) Detail of acellular cementum-like mineralized tissue. Note the absence of osteocytic lacunar spaces. (c–f) Details of the psammomatoid structures. Note the concentric layers of mineralized material of different mineral density (arrow in d). (g–i) Overview and detail of a typical sample of maxillary FD bone shown for comparison. Note the low mineralization density and the high density of large osteocytic lacunar spaces. (f and h) Pseudocolored versions of panels e and g, respectively. BSE signal intensity was calibrated by measuring the values obtained from monobrominated and monoiodinated dimethacrylate standards.[17] The color lookup table contains eight equal ranges as explained in the inset scale image. The value from Br is adjusted to zero and that from I to 255. The ranges of values shown, and the GDS bone (f) is within the range of normal mature bone. This contrasts with many regions of the FD reference case (h) in which values are exceptionally low, even for normal immature bone.

tracted from fresh lesional tissue or DNA from cultured stromal cells. Even after selective amplification of the putative mutated allele using a PNA-based method, with an estimated sensitivity of 1:200 cells, mutations were not detected.

Histology

Histology of new bioptic material from the jaw lesions showed a fibro-osseous pattern in which features diagnostic of FD (including recently identified ones such as osteoblast shape change and Sharpey fiber bone[14]) were not observed. Masses of acellular cementum-like material were scattered within a background of fibrous tissue with variable cellularity and vascularity (Figs. 2a–2c) but overall distinct from the typical fibrous background of FD. Psammomatoid structures (i.e., multiple round mineralized spherules with a lamellated internal structure) were frequent (Figs. 2d–2f). A similar pattern was observed in the histological material from all previous surgical procedures available for review.

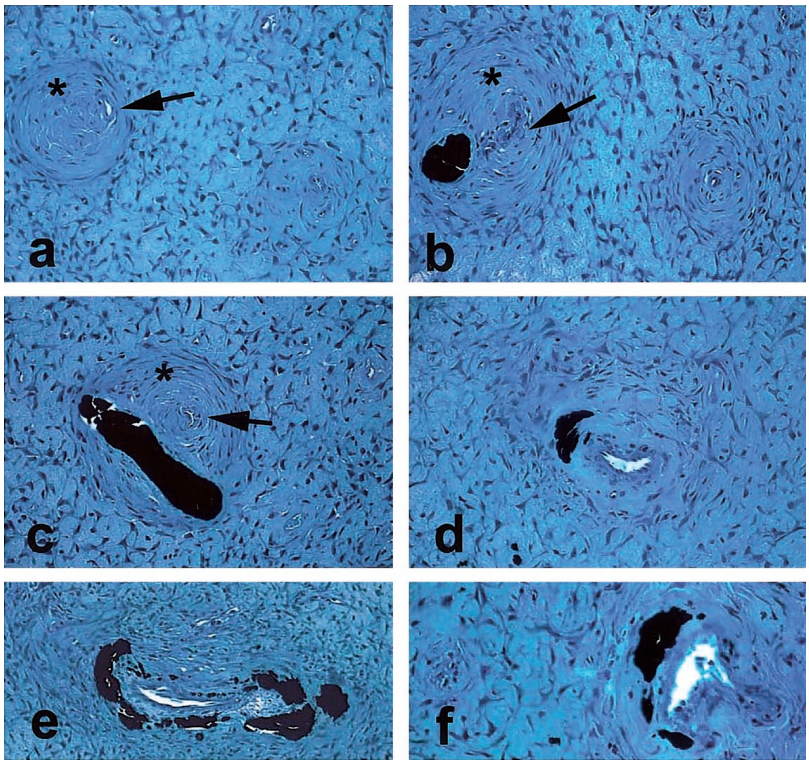

FIG. 4. Von Kossa stained, undecalcified MMA sections showing the deposition of mineralized (black) cementum-like material within the walls of abnormal blood vessels. Asterisks in a–c are for comparison with Fig. 2b, and identify blood vessels with markedly thickened ("onion-skinned") hyalinized walls. Arrows identify the narrowed lumen of the abnormal vessels. A patent lumen of the mineralized vessels is easily distinguished in d–f.

BSE microscopic analysis of the current bioptic material showed again irregular masses of cementum-like material and psammomatoid structures (Fig. 3). The latter were concentrically lamellated, focally coalescent, acellular, and contained a hypermineralized core. Masses of cementum-like material were also entirely acellular and highly mineralized (Figs. 3a–3f). These findings contrasted with the comparatively much lower mineralization and high cellularity of a typical FD bone sample from a typical GNAS1 mutation–positive patient, which is presented for comparison (Figs. 3g–3i). Based on these observations the diagnosis of psammomatoid cemento-ossifying fibroma of the jawbones was made.

Further study of the histology of the maxillary lesion showed unusual features that are either general—and hitherto unrecognized—features of cemento-ossifying fibroma at large or perhaps unique to the lesion observed in this patient. Study of undecalcified MMA sections surprisingly showed that most of the calcified material corresponding to the cementum-like structures represented aberrant calcification of thickened, hyalinized vascular walls (Figs. 4a–4f).

Immunohistochemical staining showed the presence of α-SM actin-expressing fibroblasts (myofibroblasts) in the context of the fibrous tissue (Fig. 5a), and also disclosed an unusual pattern of "disintegration" of the muscle coat of intralesional vessels (Fig. 5b). Here, aberrant expression of MMP-2 (Figs. 5c and 5d), which is known to occur in growing or regressing blood vessels,[20] also was observed.

Stromal cell transplantation into immunocompromised mice

Stromal cell strains were isolated in culture from the bioptic material obtained from the jawbone lesions. After expansion in culture, the stromal cell strains were transplanted into the subcutis of immunocompromised mice to determine their ability to form normal bone and marrow or to recapitulate an abnormal fibro-osseous tissue. Harvested 8 week posttransplant, the ectopic "ossicles" formed by the lesional cells consisted of extensive fibrous tissue and scanty amounts of bone (Fig. 6a). No hematopoietic marrow was formed. It was noted that the bonelike material formed by the lesional cells often was distributed away from the carrier surfaces and organized in spheroidal structures residing within the fibrous tissue (Figs. 6b–6d). Some of these structures were generally reminiscent of the "psammomatoid" structures observed in the native lesion. Transplanted cells from an age-matched normal donor that were used as a control formed new bone on the surface of the ceramic carrier and supported the formation of a hematopoietic marrow as was shown previously (data not shown).

DISCUSSION

Distinguishing true FD from its genetically unrelated mimics has multiple clinical implications, ranging from the need to assess carefully the endocrine status and overall skeletal metabolism of individual patients to therapeutic

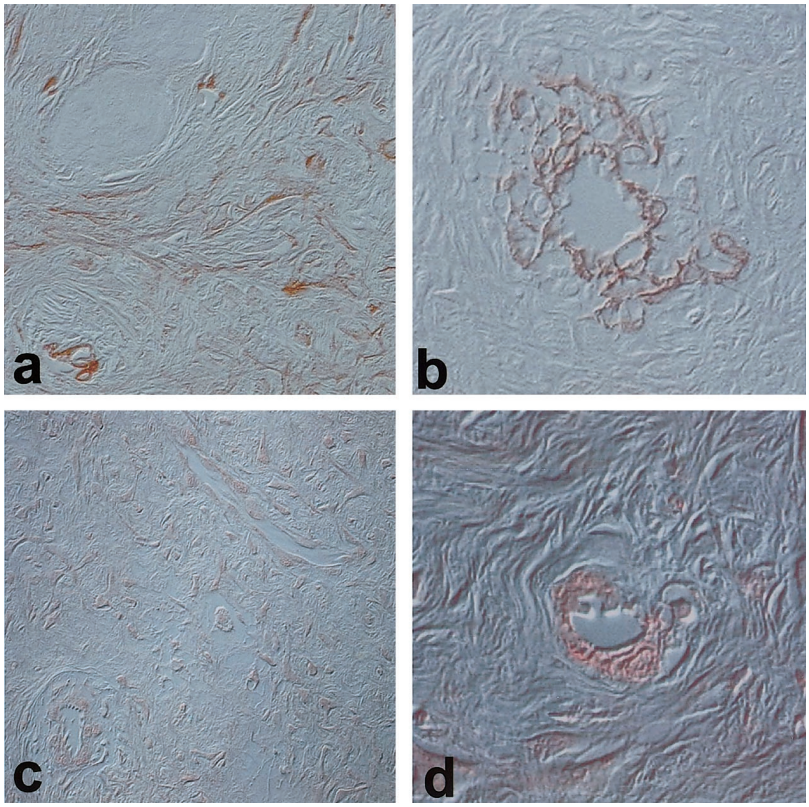

FIG. 5. Immunohistochemistry of the jaw-bone lesion. (a) α-SM actin was expressed in the fibroblast-like cells within the fibrous tissue. (b) The lacelike pattern observed within the intralesional vessels suggests disintegration of the muscular coat. (c and d) Immunolocalization of MMP-2 was observed in the fibrous component as well as in the blood vessel wall.

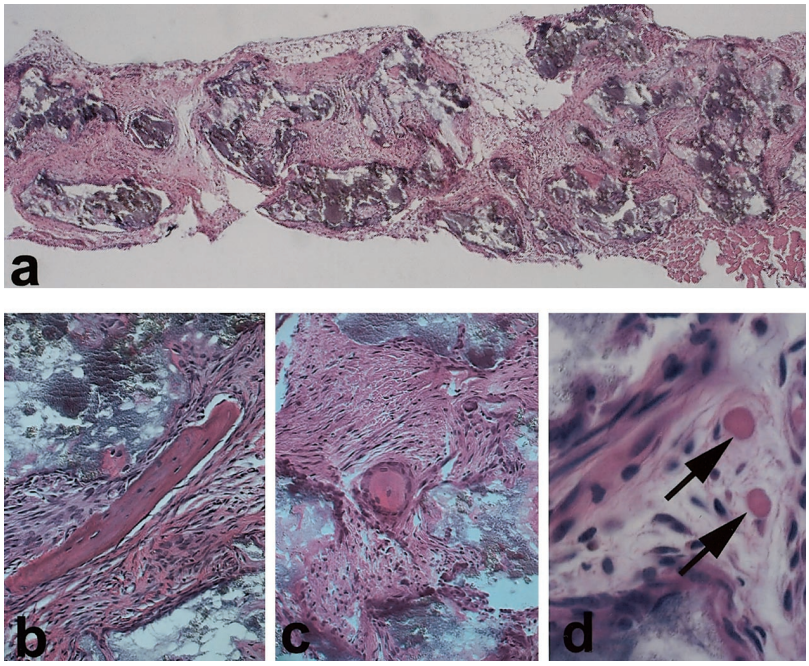

FIG. 6. In vivo transplantation assay. (a) The low power magnification of the "ossicle" formed by the lesional cells, which were expanded in culture and transplanted into the subcutis of immunocompromised mice. (b) At higher magnification, hematopoietic marrow was found to be absent and newly formed bone was scarce. (c) Spheroidal cellular or (d) acellular structures, highly reminiscent of the psammomatoid-like bodies observed in the native lesion, also were observed.

options to the low yet defined risk of malignant transformation linked to GNAS1 mutations.[21] These considerations suggest the need to attain a molecular diagnosis of FD whenever possible, especially in cases with atypical clinical findings. However, as this case exemplifies, a careful consideration of subtle histological characteristics of FD (osteoblast shape change, Sharpey fibers, and hyperosteocytosis[14]) also has a significant diagnostic impact.

In the case reported here, clinical, histological, and molecular data concurred in ruling out the diagnosis of FD. Clinically, the absence of radiological changes typical of FD, as well as the absence of skin pigmentation or endocrinopathies, made the diagnosis of FD/MAS unlikely. Furthermore, there were no significant changes in biochemical markers of bone metabolism. A sustained elevation of markers of bone formation and bone resorption is, in contrast, common in FD.[22] Histologically, the jaw lesions could be classified as cemento-ossifying fibroma[1] rather than FD. Activating missense mutations of the GNAS1 gene (R201C and R201H) are associated consistently with all forms of FD of bone, whether occurring in the context of the MAS or as polyostotic disease in the absence of endocrine changes or as isolated monostotic lesions.[13] Thus, detection of GNAS1 mutations in lesional tissue or in cells derived from it can be used as an important diagnostic aid in identifying FD of bone. Molecular analysis failed to show GNAS1 mutations in the case presented here. Therefore, it was felt that the observed maxillary lesions represented an instance of a genuine, GNAS1-R201 mutation–free, non-FD fibro-osseous lesion. The recognition of even an individual such case indicates the need to avoid the blurring of the boundary between FD and partially similar but genetically distinct fibro-osseous lesions. These include ossifying and cemento-ossifying fibromas of jawbones, and clinicopathological variants thereof. The tendency to regard FD and these non-FD fibro-osseous lesions as variants of an essentially single entity has gained broad acceptance in recent years.[12] In contrast, as this case highlights, a clear distinction between GNAS1 mutation–positive FD and GNAS1 mutation–free (and histologically similar yet distinct) fibro-osseous lesions remains important in view of its general and applicative implications.

In our case, a detailed study of the histology of the jaw fibro-osseous lesions disclosed a few previously unrecognized features of the pathological entity known as psammomatoid cemento-ossifying fibroma. Perhaps the most surprising finding was the presentation of evidence that a large proportion of the cementum-like mineralized structures appeared to be located within thickened walls of intralesional arteries (Figs. 3 and 4). This was made apparent by the use of MMA sections (Fig. 4) in which mineral is preserved and a resolution advantage is gained from the ability to cut sections at a nominal thickness of 3 μm. In conjunction with this observation, we also noted by immunolabeling that many of the intralesional arteries showed an apparent disruption of the muscle coat. Abundant cells with a fibroblastic appearance but expressing the smooth muscle marker α-SM actin were seen in the adjacent fibrous tissue. In general, detection of α-SM actin within cells of otherwise fibroblastic morphology usually is taken to identify myofibroblasts at the light microscopy level. This cell type, abundant in reparative tissues and in several lesions of extraskeletal organs,[23] has not been reported, to the best of our knowledge, in any benign fibro-osseous lesion of the skeleton. In this case, the detection of "fibroblastic" cells expressing α-SM actin around blood vessels noted for changes in their muscle coats might suggest their potential derivation from the degenerating vascular wall. We also observed the expression of MMP-2 within the lesional vascular walls (Fig. 5). Although MMP-2 normally is not observed in steady-state blood vessel walls, it is known to be expressed during phases of angiogenesis and also of regressive vascular changes.[20] Taken together, these observations raise the point whether vascular changes have a pathogenic significance in cemento-ossifying fibromas of the jaws, which would be a novel way to view these elusive pathological entities. At this time, we cannot determine whether these observations apply to the lesion type at large (i.e., to all so-called cemento-ossifying fibromas) or specifically to the single case presented here, in which, as detailed in the following paragraph, the jawbone lesions occurred within the context of an unusual systemic skeletal syndrome.

In the case presented here, ruling out the diagnosis of FD also imposed the need to reconsider the nature of the changes in the peripheral skeleton. Although repeated fractures are relatively common in FD, typical FD was never indicated radiographically in any of the bones that fractured. The long bones of the limbs also exhibited diaphyseal cortical thickening and bowing, findings that are not a feature of FD. The association of bone fragility, bowing/cortical thickening/undermodeling of tubular bones, and fibro-osseous lesions of craniofacial bones has been reported in several kindreds as an autosomally inherited trait.[24,25] A similar syndrome also has been reported as occurring sporadically.[7,26,27] Some degree of phenotypic variability occurs across different patients that have been regarded as examples of this syndrome. We believe that our patient represents a further instance of this poorly characterized syndromic association. Our patient exhibits the type of jaw lesions, long bone abnormality, and fracture diathesis described previously by Akasaka et al.,[24] Leven et al.,[25] Colavita et al.,[27] and by Nishimura et al. (cases 1 and 2).[26] Previous hypotheses as to the nature of this unusual syndrome have included a specific and as yet uncharacterized variety of osteogenesis imperfecta (OI). However, the potential underlying gene defect has never been identified in these patients. Based on this and the lack of typical clinical features of OI in the reported cases, bone fragility remains the only possible association to OI, a link that is tenuous at best. Akasaka et al.[24] proposed the term "gnathodiaphyseal sclerosis" for this entity. Because sclerosis is not a feature of the jawbone lesions and is an inaccurate way of conveying the cortical thickening of long bones, we propose the substitute label of "gnathodiaphyseal dysplasia." This term also emphasizes the likely congenital character of the disorder itself, if not of the individual lesions, and their surmised developmental nature. The potential underlying genetic substrate remains an interesting challenge. We observed that the ability of the lesional cells to form psammomatoid structures—a histological hallmark of the lesion—was retained on their transplantation in immunocompromised mice. In this respect, in the transplantation assay the lesional cells behaved as skeletal stromal cells carrying known (natural or targeted) genetic changes; that is, they recapitulate the lesion from which they are derived.[13,18,28,29] This suggests that the phenotypic property of generating a fibro-

osseous tissue with abnormal mineralizing structures is inherent to the lesional cells, which would be consistent with an as yet undefined genetic trait.

ACKNOWLEDGMENTS

This work was supported by Telethon Fondazione Onlus Grant E1029 (P.B.).

REFERENCES

1. Slootweg PJ 1996 Maxillofacial fibro-osseous lesions: Classification and differential diagnosis. Semin Diagn Pathol **13:** 104–112.
2. Posnick J 1998 Fibrous dysplasia of the craniomaxillofacial region: Current clinical perspectives. Br J Oral Maxillofac Surg **36:**264–273.
3. Eversole LR, Sabes WR, Rovin S 1972 Fibrous dysplasia: A nosologic problem in the diagnosis of fibro-osseous lesions of the jaws. J Oral Pathol **1:**189–220.
4. Camilleri AE 1991 Craniofacial fibrous dysplasia. J Laryngol Otol **105:**662–666.
5. Boysen ME, Olving JH, Vatne K, Koppang HS 1979 Fibro-osseous lesions of the cranio-facial bones. J Laryngol Otol **93:**793–807.
6. Eversole LR, Leider AS, Nelson K 1985 Ossifying fibroma: A clinico pathologic study of sixty-four cases. Oral Surg **60:**505–511.
7. Levine P, Wiggins R, Archibald RW, Britt R 1981 Ossifying fibroma of the head and neck: Involvement of the temporal bone. An unusual and challenging site. Laryngoscope **9:**720–725.
8. Margo CE, Ragsdale BD, Perman KI, Zimmerman LE, Sweet DE 1985 Psammomatoid (juvenile) ossifying fibroma of the orbit. Ophthalmology **92:**150–159.
9. Marvel JB, Marsh MA, Catlin FI 1991 Ossifying fibroma of the mid-face and paranasal sinuses: Diagnostic and therapeutic considerations. Otolaryngol Head Neck Surg **104:**803–808.
10. Montgomery AH 1927 Ossifyng fibroma of the jaw. Arch Surg **15:**30–44.
11. Summerlin DJ, Tomich CE 1994 Focal cemento-osseous dysplasia: A clinicopathologic study of 221 cases. Oral Surg Oral Med Oral Pathol **78:**611–620.
12. Voytek TM, Ro JY, Edeiken J, Ayala AG 1995 Fibrous dysplasia and cemento-ossifying fibroma. A histologic spectrum. Am J Surg Pathol **19:**775–781.
13. Bianco P, Riminucci M, Majolagbe A, Kuznetsov SA, Collins MT, Mankani MH, Corsi A, Bone HG, Wientroub S, Spiegel AM, Fisher LW, Gehron Robey P 2000 Mutation of the GNAS1 gene, stromal cell disfunction and osteomalacic changes in non-McCune-Albright fibrous dysplasia of bone. J Bone Miner Res **15:**120–128.
14. Riminucci M, Liu B, Corsi A, Shenker A, Spiegel AM, Robey PG, Bianco P 1999 The histopathology of fibrous dysplasia of bone in patients with activating mutations of the Gs alpha gene: Site-specific patterns and recurrent histological hallmarks. J Pathol **187:**249–258.
15. Riminucci M, Fisher LW, Majolagbe A, Corsi A, Lala R, De Sanctis C, Robey PG, Bianco P 1999 A novel GNAS1 mutation, R201G, in McCune-albright syndrome. J Bone Miner Res **14:**1987–1999.
16. Riminucci M, Fisher LW, Shenker A, Spiegel AM, Bianco P, Gehron Robey P 1997 Fibrous dysplasia of bone in the McCune-Albright syndrome: Abnormalities in bone formation. Am J Pathol **151:**1587–1600.
17. Boyde A, Travers R, Glorieux FH, Jones SJ 1999 The mineralisation density of iliac crest bone from children with osteogenesis imperfecta. Calcif Tissue Int **64:**185–190.
18. Bianco P, Kuznetsov SA, Riminucci M, Fisher LW, Spiegel AM, Robey PG 1998 Reproduction of human fibrous dysplasia of bone in immunocompromised mice by transplanted mosaics of normal and Gs alpha-mutated skeletal progenitor cells. J Clin Invest **101:**1737–1744.
19. Krebsbach PH, Kuznetsov SA, Satomura K, Emmons RV, Rowe DW, Robey PG 1997 Bone formation in vivo: Comparison of osteogenesis by transplanted mouse and human marrow stromal fibroblasts. Transplantation **63:**1059–1069.
20. Sakalihasan N, Delvenne P, Nusgens BV, Limet R, Lapiere CM 1996 Activated forms of MMP2 and MMP9 in abdominal aortic aneurysms. J Vasc Surg **24:**127–133.
21. Ruggieri P, Sim FH, Bond JR, Unni KK 1994 Malignancies in fibrous dysplasia. Cancer **73:**1411–1424.
22. Collins MT, Chebli C, Jones JM, Kushner H, Consugar M, Rinaldo P, Wientroub S, Bianco P, Robey PG 2001 Renal phosphate wasting in fibrous dysplasia of bone is part of a generalized tubular dysfunction similar to that seen in tumor-induced osteomalacia. J Bone Miner Res **16:**803–813.
23. Schmitt-Graff A, Skalli O, Gabbiani G 1989 Alpha-smooth muscle actin is expressed in a subset of bone marrow stromal cells in normal and pathological conditions. Virchows Arch B Cell Pathol Mol Pathol **57:**291–302.
24. Akasaka Y, Nakajima T, Koyama K, Furuya K, Mitsuka Y 1969 Familial cases of a new systemic bone disease, hereditary gnatho-diaphyseal sclerosis. Nippon Seikeigeka Gakkai Zasshi **43:**381–394.
25. Levin LS, Wright JM, Byrd DL, Greenway G, Dorst JP, Irani RN, Pyeritz RE, Young RJ, Laspia CL 1985 Osteogenesis imperfecta with unusual skeletal lesions: Report of three families. Am J Med Genet **21:**257–269.
26. Nishimura G, Haga N, Ikeuchi S, Yamaguchi T, Aoki K, Yamato M 1996 Fragile bone syndrome associated with craniognathic fibro-osseous lesions and abnormal modeling of the tubular bones: Report of two cases and review of the literature. Skeletal Radiol **25:**717–722.
27. Colavita N, Kozlowski K, La Vecchia G, Fileni A, Ricci R 1984 Calvarial doughnut lesions with osteoporosis, multiple fractures, dentinogenesis imperfecta and tumorous changes in the jaw. Aust Radiol **28:**226–231.
28. Holmbeck K, Bianco P, Caterina J, Yamada S, Kromer M, Kuznetsov SA, Mankani M, Robey PG, Poole AR, Pidoux I, Ward JM, Birkedal-Hansen H 1999 MT1-MMP-deficient mice develop dwarfism, osteopenia, arthritis, and connective tissue disease due to inadequate collagen turnover. Cell **99:**81–92.
29. Bianco P, Robey P 1999 Diseases of bone and the stromal cell lineage. J Bone Miner Res **14:**336–341.

Address reprint requests to:
Pamela Gehron Robey, Ph.D.
30 Convent Drive
MSC 4320
Bethesda, MD 20892, USA